On the high-rate failure of carbon fibre composites

DOI:
10.1063/1.4971674

Document Version
Final published version

Published in:
SHOCK COMPRESSION OF CONDENSED MATTER

On the high-rate failure of carbon fibre composites

C. Frias, S. Parry, N. K. Bourne, D. Townsend, C. Soutis, and P. J. Withers

Citation: **1793**, 110011 (2017); doi: 10.1063/1.4971674
View online: http://dx.doi.org/10.1063/1.4971674
View Table of Contents: http://aip.scitation.org/toc/apc/1793/1
Published by the American Institute of Physics

On the high-rate failure of carbon fibre composites

C. Frias[1], S. Parry[2, 3], N.K. Bourne[2, 1, a], D. Townsend[2], C. Soutis[1], P.J. Withers[1]

[1]*School of Materials, University of Manchester, Manchester, M13 9PL, UK.*
[2]*CMEC, University of Manchester, Rutherford Appleton Laboratory, Didcot, Oxfordshire, OX11 0FA.*
[3]*Defence Science and Technology Organisation, PO Box 1500, SA 5111, Australia.*
[a)]Corresponding author: neil.bourne@manchester.ac.uk

Abstract. The Taylor test is an important means to determine the response of materials to dynamic loading. In this work it is used to determine the dynamic response of heterogeneous orthotropic carbon-fibre-epoxy laminates. Experiments record the fracture of a series of multi-layered composite plates with high-speed photography. The ensuing damage occurs during the shock compression phase but three other tensile and shear loading modes operate during the test. This hierarchy of damage across the scales is key in determining the suite of operating mechanisms; such information cannot be correlated using traditional sectioning and observation using optical or electron beam microscopy or post mortem examination of recovered cylinders. Only dynamic imaging and damage characterisation will advance quantitative damage and thus constitutive model development. It is shown that fibre and ply orientations influence the fracture response, but most important is the impact speed. The 0° Taylor cylinder impacted at 268 m s^{-1} in addition to extensive interlaminar fracture demonstrates a pseudo-plastic behaviour due to progressive fibre crushing, dissipating larger amounts of energy in comparison to that tested at the lower speed of 148 m s^{-1}.

1. INTRODUCTION

Understanding damage to (and failure of) composite materials is critical for reliable and cost-effective engineering design. Damage within composites can take a range of different modes according to load and architecture including cracking, breakage and buckling [1]. These macroscale responses result from microscale processes operating at mesoscale material interfaces and thus a suite of physical mechanisms underlie the nucleation and progression of damage under mechanical loads [2].

The Taylor test offers a mesoscale geometry in which different mechanisms at different length scales operate within the microstructure and lead to a macroscopic response conditioned by both macroscale inertial constraints and mesoscale damage mechanics [3, 4]. Operating mesoscale mechanisms in the composites considered here include the nucleation of matrix fracture at defects which starts debonding, leading then to fibre delamination and subsequently fracture [2]. The modern adaptation of the Taylor test is a fully integrated experiment that not only records the macroscopic behaviour but allows interrogation of these mesoscale physical mechanisms. It has been extensively used in constitutive model validation for metals but not for other classes of material [5]. In particular after a loading phase that is first controlled by compression and viscoplastic flow, there is a second which follows with release and fracture. This latter phase affords a means of studying three independent modes of tensile failure in one geometry and shows distinct regions of deformation that are separated in position and in time. The head of the rod, and only a central conical portion of it, experiences a shocked state. In this phase of the loading the global stress state is inhomogeneous. Within one diameter of the impact face, the loading front has exited this one-dimensional strain state and entered an axisymmetric loading phase dominated by a decaying elastic front travelling towards the rear of the cylinder which reveals behaviour that results from the macroscopic one dimensional stress state within the rods. The loading modes and their different nature and effect are discussed elsewhere [6].

2. MATERIALS AND EXPERIMENTS

The composite panel was constructed from autoclave-cured, pre-impregnated (pre-preg) sheets, made from unidirectional, intermediate modulus carbon fibres encased within a toughened epoxy. These pre-preg sheets (~0.125 mm) were layered in 0° and 90° orientations, $[0_m/90_m]_{ns}$ cross-ply laminate, to a final panel thickness of approximately 25 mm. Right cylinders were machined in the in-plane 0°, 45º and through-thickness (TT)

Shock Compression of Condensed Matter - 2015
AIP Conf. Proc. 1793, 110011-1–110011-4; doi: 10.1063/1.4971674
Published by AIP Publishing. 978-0-7354-1457-0/$30.00

orientations from the panel. Taylor tests were performed on these composite cylinders and had a diameter of 7.6 mm, a length of 22.5 mm or 38.0 mm and a mass of *ca*. 1.6-2.7 g giving an approximate length to diameter ratio of 3:1 or 5:1. The cylinders were fired from a single stage gas gun using helium or nitrogen driver gases. Impact was onto a hardened steel anvil and targets were aligned for normal impact to within 10 mrad to controlled impact. Molybdenum disulphide (MoS_2) grease was applied to the surface of the anvil to reduce friction at the impact face. A digital high-speed camera (Vision Research Phantom V12), operating at 120,000 frames per second and with a 1 μs frame exposure time (ET), was used to record the events. The interframe time (IFT) for the reproduced frames is indicated on the sequences.

3. HIGH SPEED IMAGING OF IMPACT

In the following sections the impact responses of Taylor cylinders impacting a rigid anvil are shown for a range of impact velocities and for the three cuts of cylinder described. In all cases a range of impacts with speeds in the range from below 100 to above 300 m s^{-1} was conducted in order to cover the failure modes observed in the composite. Selected sequences typical of the observed behaviours are shown here.

Fig. 1 shows two impacts at 148 and 268 m s^{-1} conducted on the 0˚ sample. The lower speed sequence in a). is above the first damage threshold for the material which is around 50 m s^{-1}. The sequences shown have IFT 33 μs in each case. The impact in frame 3 is symmetrical and initial delamination starts in the first frames. The first indication of fibre-end fracture against the surface of the anvil can be seen. The failure of these fibres, particularly in the outermost region, creates a surface fragment field with submillimetre fibre remnants visible at the anvil surface. However most of the impact energy is taken in matrix fracture and in delamination by interlaminar shear. In this particular case the elastic deformation of the left most fibres bends and then releases the outer fibres springing this region back off the surface and rotating the remaining damaged cylinder at the surface zone. This asymmetry meant that delamination did not continue to the rear surface on the LHS whilst the freeing surface on the RHS allows delamination to just reach the rear surface for the outermost plies. On frame two of the sequence is superposed two axes (*x* and *y*) onto one image of the cylinder. These represent two axes for the impact for which streak images have been taken and shown to the right of the framing sequence. The central *x*-*t* image shows the intrusion of the rod onto the impact surface and its diameter spreading for the contact time with fragments flowing outward from the impact zone. The *y*-*t* (furthest right) shows the rod entering the field of view, impact on the surface, return of the wave from the impact face. It shows that the rear of the rod has initially rebounded from the surface but then rotation within a diameter of the surface for the remaining time. For a fully three-dimensional loading geometry this 1D projection cannot interrogate all phases of loading on the anvil. However it allows a valuable quantitative picture of interface and wave behaviour to be obtained for these materials.

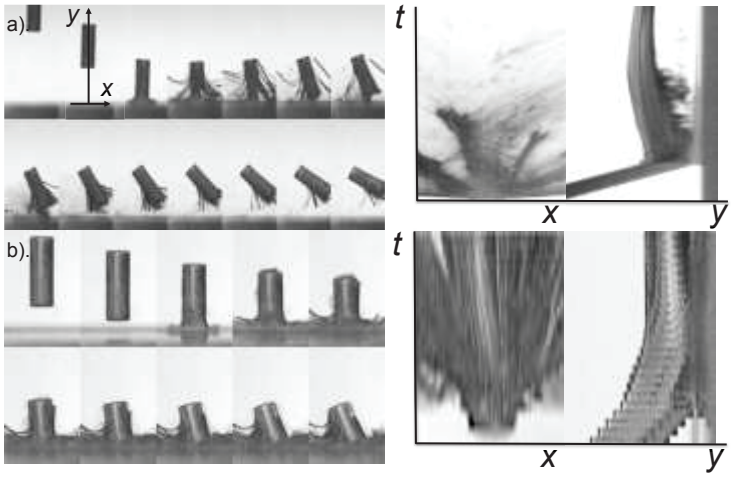

FIGURE 1. Impact onto 0˚ composite Taylor cylinders. a). impacts 148 & b). 268 m s^{-1}. IFT 33 μs. Streak (*x*-*t*) images to right.

Fig. 1 b). shows the impact of a cylinder from the same 0˚ cut at 268 m s^{-1} and although there is qualitatively similar delamination and interlaminar shear response to that seen in the lower speed sequence, the macroscopic behaviour is more homogeneous. This stress level represents a further threshold in micromechanical behaviour for the material under load. There is now more uniform surface damage to the rod with buckling and failure of all the fibres within 1D of the impact face. Further, interlaminar failure just propagates to the rear of the cylinder on all

planes (although this rod is L/D=3 and thus shorter than that in a). However at this speed there is also fibre fracture on the surface and also delamination within the central core where material is inertially confined.

The central x-t streak shows the intrusion of the rod onto the impact surface but now deformation is localized and uniform across the surface zone. Some evidence of the flow of outer parts of the core at greater diameters is evident at later times. The y-t streak shows the rod entering, impact on the surface and an inelastic flow region for deformation and finally, rest of the remnant cylinder onto the surface. It illustrates that this speed represents a threshold beyond which a pseudo-hydrodynamic response for this composite structure maybe be used to describe response. A macroscopic continuum mechanics based constitutive model is presented in a companion paper [7].

Fig. 2. shows the impact of a 45˚ laminate at 213 m s^{-1}. The response illustrated here is qualitatively similar to that at other speeds over the velocity range considered. The impact causes immediate delamination of the incoming composite panel; since the principal operating deformation mechanism is shear-induced microfracture the 45˚ layup leads to easy delamination and flow for the composite under impact. The first diameter (subject to the highest stresses) fails and flows easily over the first frames. Very quickly there is failure down the confined core fibre region (which required much higher velocities in the case of the 0˚ case) and fracture extends more easily back to the rear surface opening two hinged struts that rapidly collapse the bulk of the material onto the surface accommodating the impact energy in flow across the rigid surface. There is little debris ejected around the site as in the other sequences with fibres large intact, showing the easy of delamination in this geometry relative to other modes of failure and less energy is expanded in fibre crushing and fracture.

The x-streak image shows easy break up and surface flow relative to the more inhomogeneous and extended failure for the 0˚ case despite the impact velocity in that case being 25% greater (and thus the input kinetic energy being *ca.* 60% more). The y-streak shows graphically the macroscopic response of the cylinder in this geometry as it impacts and then collapses and flows across the anvil.

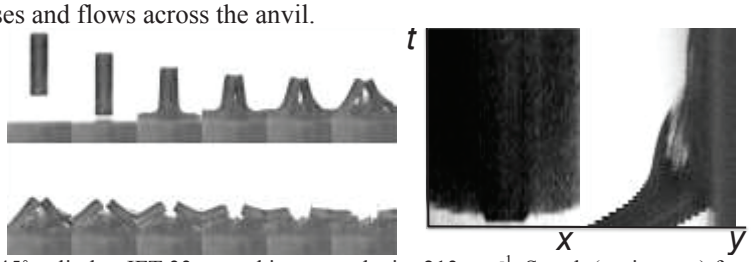

FIGURE 2. Impact onto 45˚ cylinder; IFT 33 μs and impact velocity 213 m s^{-1}. Streak (x-t images) for the x and y axes to right.

Finally Fig. 3 shows the response of cylinders cut in the TT direction to impact in this geometry. Fig. 3 a). shows an impact at the lower speed of 153 m s^{-1} with around the same kinetic energy as that of Fig. 1 a). The response is however very different to either of the other cut directions shown. Frame 7 shows a puff of dust as the epoxy laminate fails expelled outwards to the right as the first failure occurs at slightly less then one diameter from the impact face. This corresponds to the end of the shocked zone in the composite. Later frames show that this corresponds to the failure of the surface impact plug and also a single adjacent ply at this position that is seen detaching (and rotating) through subsequent frames. Of course a release fan propagates from rod surfaces and this will disperse tensile loading across several fibre planes. There is a sparse population of damaged fibres seen expelled in crushing at the impact face and also in the vicinity of the delamination plane in this geometry. These amount to a few isolated fibres that have little momentum and whose ejection absorbs negligible energy.

The anvil face x streak shows graphically that the impact and rebound is largely elastic. There is little expansion of the cylinder on the surface and the grey areas correspond to ejected grease not failed material in this image. The y axis streak on the other hand indicates the almost rigid body nature of the impact and graphically illustrates the response of the composite. The rear two diameter length segment of the cylinder rebound elastically as can be seen whilst the expelled rotating disc and the surface plug travel more slowly from the surface. The rear of the cylinder shows a change in slope on the return of the compression wave from the impact face and a subsequent slight deceleration of the cylinder on the rebound. This impact speed represents a critical onset of interlaminar fracture in the cylinder and occurs behind the zone of compression that exists on the surface.

Fig. 3 b). shows the response when a much higher impact pressure is induced and the composite is unzipped into a stack of failed discs by wave interactions in the stack. The shocked surface zone and now the rest of the incoming column have interply regions rapidly failed by the returning compression wave which then reflects as an elastic tensile pulse. As seen earlier this does not fail the original as-received material but clearly now unzips the cylinder into a stack of adjacent failed plies. The greatest velocity is imparted to that zone where the release reaches first and the ejected disc traps most of the momentum within it bouncing back at almost the incoming rod speed. Further

discs gradually receive less of the returning impulse as the wave decays down the stack expending energy failing the zone damaged in compression. The *x* streak for the impact shows little lateral expansion on the anvil surface (as was the case for the lower speed impact) yet a cloud of failed fibres and grease from the impact can be seen emanating from the impact zone. The *y* streak shows very graphically the expanding stack of discs under the returning release front from the rear surface. The top of the upper fragment seen here has almost the same speed as the incoming cylinder and the slowing velocity of each stack reflects energy expended in failing planes down the stack as the cylinder fragments. The larger fragments are at the rear of the rod where the compression wave has induced less damage and the greater failure and fragmentation is in the surface zone as expected. There is little or no rear surface ejecta but there are sprays of failed epoxy from the opening composite planes expelled laterally during impact. Nevertheless there is little inelasticity seen in any of the rapid interlaminar failures.

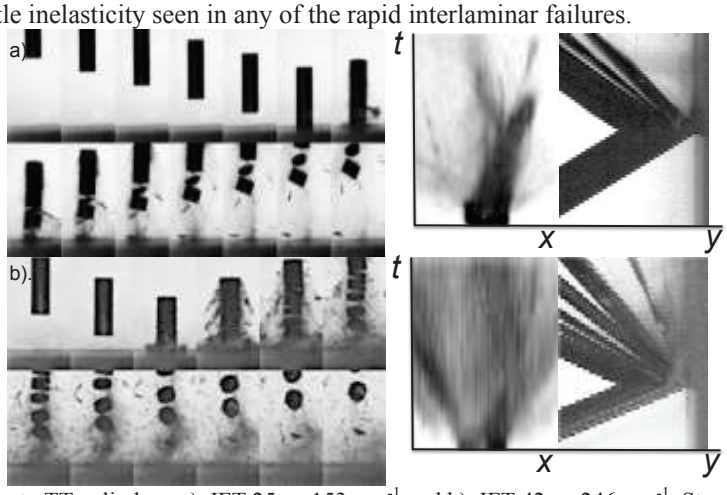

FIGURE 3. Impacts onto TT cylinders. a). IFT 25 μs 153 m s^{-1} and b). IFT 42 μs 246 m s^{-1}. Streak (*x*-*t*) images to right.

4. DISCUSSION AND CONCLUSIONS

The Taylor test is a useful descriptor for failure and a rigorous test of constitutive models for composite response in compression, tension and shear [5]. Careful design of the velocities and geometries of the loading allows composite damage to be localised by design by using release interactions to probe weak interfaces within the microstructure. This work has shown that rods cut down varying directions in an orthotropic material show varying response to a simple applied loading on a rigid anvil. Experiment has shown that ply orientations respond to two release components; longitudinal and radial as well as the hoop stresses generated in inelastic flow at the impact surface. The through-thickness direction fails entirely down the length into platelets at damage planes induced down the impact axis. In the in-plane geometry however, damage initiates after lateral release in the first diameter and fractures the cylinder by interlaminar debonding. The test can rank different failure mechanisms in a loaded composite across all modes of loading and as such can be used to discriminate between new structural composite designs as well as in validation of numerical simulations using new constitutive descriptions of composites [7]. Coupled with dynamic and tomographic identification of failure, the technique is being relaunched as a quantitative dynamic failure test for composites to determine operating mechanisms, screen new composite layups and observe macroscopic high-rate response as well as serving its principal use in recent times in validating the most modern constitutive descriptions.

REFERENCES

1. J.D.H. Hughes, Composites Science and Technology, **41**, (1991), 13-45.
2. P.M. Jelf and N.A. Fleck, J. Composite Materials, **26**, 2706-2726, (1992).
3. G.I. Taylor, Proc. Roy. Soc. London A 194, 289 (1948).
4. R.L. Woodward, N.W. Burman and B.J. Baxter, Int. J. Impact Engineering, **15**, 4 (1994).
5. P.J. Maudlin, G.T. Gray III, C.M. Cady, G.C. Kaschner, Phil. Trans. R. Soc. Lond. A **357**, 1707-1729,
6. N.K. Bourne, *Materials in Mechanical Extremes: Fundamentals and Applications*: CUP, (2013).
7. A.D. Resnyansky, S. Parry, N.K. Bourne, D. Townsend, B. James, in SCCM 2015, AIP, in press, (2015).